EurJOC
European Journal of Organic Chemistry

Research Article
doi.org/10.1002/ejoc.202101333

Chemistry Europe
European Chemical Societies Publishing

www.eurjoc.org

Special Collection

A Tetracyanobutadiene Spirobifluorene: Synthesis, Enantiomeric Resolution and Chiroptical Properties

Ani Ozcelik,[a] Raquel Pereira-Cameselle,[a] Ángeles Peña-Gallego,*[b] and J. Lorenzo Alonso-Gómez*[a]

In memory of François Diederich

Push-pull organic compounds with π-conjugated backbones are attracting considerable interest in terms of their highly efficient (NLO) non-linear optical effects. In this respect, cyano groups constitute one of the strongest electron acceptors suitable for NLO materials. We herein report the first 1,1,4,4-tetracyanobutadiene (TCBD) spirobifluorene (SBF) through a double [2 + 2] cycloaddition-retroelectrocyclization. Enantiomeric resolution by HPLC using a chiral stationary phase (CSP) and theoretical calculations unveiled not only the nature of the potential energy surface, but also the absolute configuration of each enantiomer. Since both the presence of strong donor and acceptor, as well as the intrinsic non-centrosymmetric character of chiral compounds are a prerequisite for the development of NLO properties, the first hyperpolarizability of the developed system was theoretically calculated. The results suggested a strong dependence on the conformation and an intensity enhancement for certain conformers of **1** as compared to its allenic TCBD analogue. Therefore, the present study opens a new class of SBF compounds suitable for NLO applications.

Introduction

Organic molecules bearing donor and acceptor groups linked by π fragments[1,2] have been in pursuit of materials with large NLO properties.[3–7] Studies have similarly indicated the relevance of chirality toward NLO candidates.[8] On the other hand, the tetrahedral carbon atom connecting two perpendicular rings in spiranes is responsible for the 3D geometry and rigidity of these systems.[9] In the case of spirobifluorene (SBF), the 90° relative orientation between the fluorene units provides thermal stability and solubility (Figure 1).[10,11] The unique optoelectronic properties of these systems have made them useful in several applications such as polymer chemistry,[12] catalysis[13] or organic electronics.[14] While there are a total of 16 available positions assessed for the functionalization of SBFs, those substituted at the C2 position are of great interest due to their high reactivity, as well as ability to efficiently expand π-conjugation.[15] As 2,2′-disubstituted SBFs offer axial chirality, we theoretically predicted[16] and experimentally demonstrated the suitability of SBFs for the development of robust chiroptical systems including all-carbon double helices and flexible shape-persistent macrocycles,[17] chiral frameworks for surface functionalization[18] or even systems featuring helical molecular orbitals.[19]

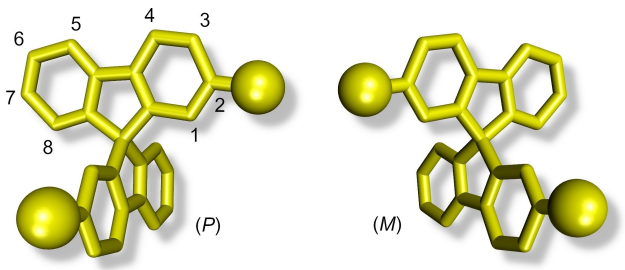

Figure 1. 3D representation of (*P*) and (*M*) stereoisomers of 2,2'-disubstituted-9,9'-spirobifluorene.

TCBD derivatives have attracted the attention of several studies for their reliability in optoelectronic applications.[20] The typical intramolecular charge transfer presented by these systems particularly reaches beyond the UV/Vis region of the electromagnetic spectrum toward the near infra-red.[21] The steric crowding in TCBDs also results in twisted conformations that improves their applicability[22] and processability.[23] In very special cases, the high energy interconversion between conformations allows for the resolution of chiral atropisomers.[24]

Diederich and Crassous have earlier reported TCBDs directly attached to chiral allenes[25,26] and helicenes,[27] respectively, to control the handedness of the twisted TCBDs (Figure 2). However, even when SBFs and TCBDs are both very useful

[a] *Dr. A. Ozcelik, Dr. R. Pereira-Cameselle, Prof. Dr. J. L. Alonso-Gómez*
Departamento de Química Orgánica,
Universidade de Vigo, Lagoas-Marcosende, Vigo 36310, Spain
E-mail: lorenzo@uvigo.es
www.smartchiralframeworks.com
[b] *Prof. Dr. Á. Peña-Gallego*
Departamento de Química Física
Universidade de Vigo, Lagoas-Marcosende, Vigo 36310, Spain
E-mail: mpena@uvigo.es

Supporting information for this article is available on the WWW under https://doi.org/10.1002/ejoc.202101333

This article belongs to a Joint Special Collection dedicated to François Diederich.

Research Article
doi.org/10.1002/ejoc.202101333

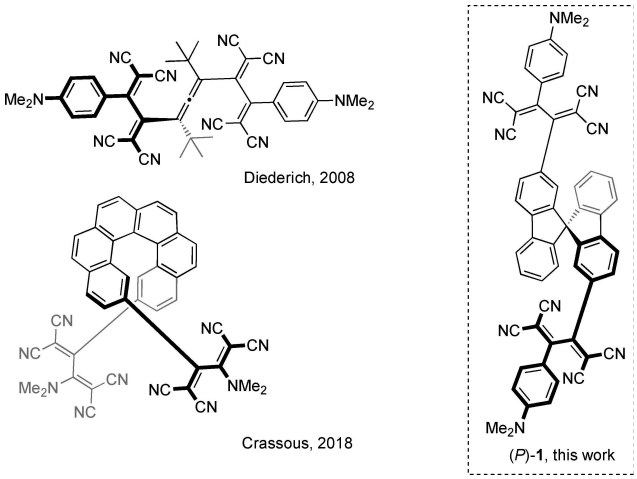

Figure 2. Structures of previously reported TCBD-allene[25,26] and TCBD-helicene,[27] and TCBD-SBF (*P*)-**1**.

moieties for the development of functional materials, no examples of TCBD-SBFs have been reported to date. Therefore, in this work we describe the synthesis, enantiomeric resolution, as well as evaluation of both optical and chiroptical properties of the first TCBD-SBF **1**. Theoretical simulations postulate that these systems can serve as promising candidates for NLO applications.

Results and Discussion

Recently published diethynyl spirobifluorene (±)-**2** bear aniline moieties directly attached to the acetilenes.[28] This fact makes them electron rich and susceptible for [2 + 2] cycloaddiotion-retroelectrocyclization. Thus, the reaction of (±)-**2** with tetracyanoethylene (TCNE) was performed in $CDCl_3$ to follow the reactivity of the acetylenes present in the system by ^{1}H NMR at 25 °C (Scheme 1). The purification and full characterization of (±)-**1** by means of ^{1}H NMR, ^{13}C NMR, and HR-ESI-MS uncovered a quantitative conversion, which is typical of this type of click reactions.[29] Thermogravimetric analysis and differential scanning calorimetry showed a thermal stability c.a. 200 °C (for more information see the Supporting Information).

The enantiomeric resolution of (±)-**1** was carried out through semi-preparative HPLC using the chiral stationary phase (Chiralpak® IA) with a 1:1 mixture of CH_2Cl_2/*n*-hexane solvent system and a flow rate of 2 mL min^{-1}. The enantiomeric excess of each fraction was determined to be over 99% (for more information, see the Supporting Information). The electronic circular dichroism (ECD) spectra were subsequently measured in CH_2Cl_2. As depicted in Figure 4, the ECD spectra present a broad band centered at 550 nm and a sharper band of opposite sign at 425. We also observed high stability for the fraction B by monitoring ECD spectra at different times of daylight exposure (for more information see the Supporting Information).

In order to evaluate the chiroptical responses, we conducted a theoretical study by first exploring the potential energy surface (PES).[30] Three torsion angles, α, β and θ, of the model system **3** bearing a single TCBD unit were analyzed (Scheme 2, for more information see the Supporting Information). Each torsion angle was scanned independently at the Hartree-Fock level of theory with STO-3G basis set, followed by full optimization of the low energy structures obtained from each PES (see Figures S13–S23 in the Supporting Information) at the B3LYP/6-31G(d,p) level of theory. The sequential exploration of the torsion angles from α rendered 3 conformers, each of which was subjected to the scanning of β, leading to 7 conformers. Finally, θ was scanned for the 7 conformers and this strategy gave a total of 14 conformers (Figure S24, for more information see the Supporting Information). The PES of (*P*)-**1** was next explored by considering the possible conformers of **3** and the relative energy window was limited to below 0.7 kcal mol^{-1}. With these characteristics, two pairs of enantiomeric conformers could be found, in which the main features are the relative orientation of the aniline moiety pointing to the neighboring fluorine or away from it and the twist of the butadiene moiety (Figure 3). These four conformations for the TCBD moiety were combined in all the possible combinations in (*P*)-**1**, giving rise to a total of 10 conformers after optimization at the B3LYP/6-31G(d,p) level of theory.

Only the three conformations with relative energies below 0.7 kcal mol^{-1} were taken into account for the prediction of UV/Vis and ECD at the CAM-B3LYP/6-31G(d,p) level of theory (Figure 4, for more details see the Supporting Information). This hybrid functional was chosen for a better definition of the excited states,[31] and solvent effects were introduced through polarizable continuum model (PCM)[32] in order to match the solvent media used for the experimental ECD and UV/Vis measurements. Theoretical spectra were then constructed by the Boltzmann distribution[33] of each low-energy conformer as a function of their Gibbs free energies (for more information see the Supporting Information). The good agreement between theoretical and experimental ECD spectra allows us to assign

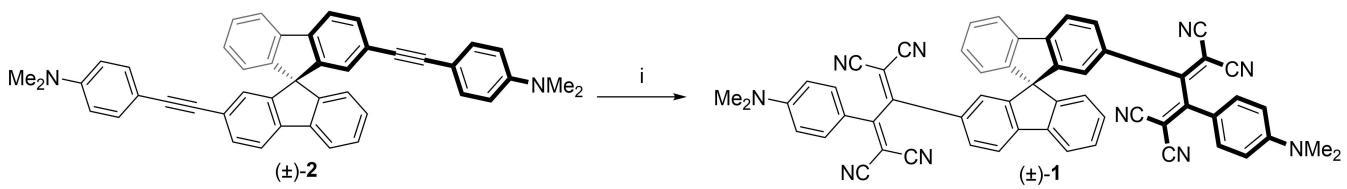

Scheme 1. Synthesis of (±)-**1** from (±)-**2**. Reagents and conditions: i) tetracyanoethylene, $CDCl_3$, 25 °C, 5 h.

Research Article
doi.org/10.1002/ejoc.202101333

Scheme 2. Methodology for systematic scan (left) and representation of the torsion angles explored for PES of model system **3** (right).

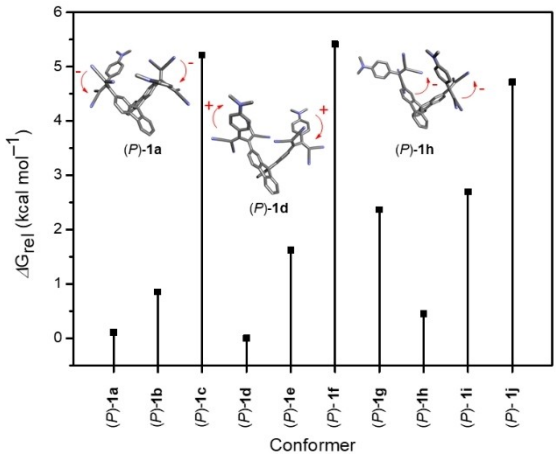

Figure 3. Relative Gibbs free energies for conformers from (*P*)-**1 a** to (*P*)-**1 j** after optimization at the B3LYP level of theory using 6-31G(d,p) basis set. Internal torsion angles adopted by tetracyanobutadiene moieties are depicted in red.

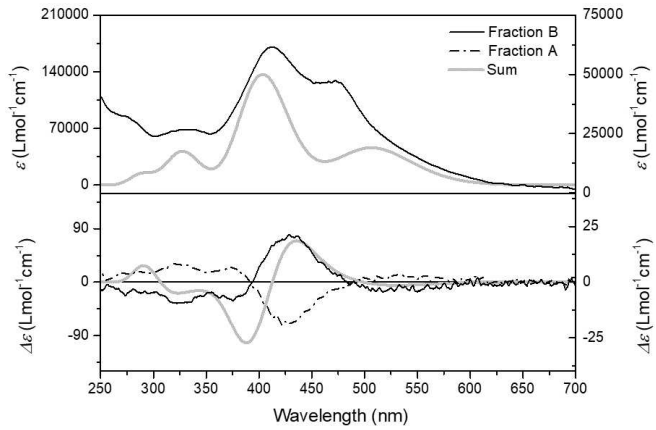

Figure 4. Comparison of theoretical Boltzmann weighted UV/Vis (top) and ECD (bottom) spectra with those of fractions A and B obtained from enantiomeric resolution of (±)-**1** measured in CH_2Cl_2. Theoretical calculations were performed at the CAM-B3LYP/6-31G(d,p) level of theory and solvent effects (CH_2Cl_2) were introduced by polarizable continuum model. For the sake of clarity, the theoretical Boltzmann weighted spectra were red-shifted by 0.39 eV and all bands were broadened with a Gaussian of HWHM = 0.20 eV. Left y-axes stand for theoretical data.

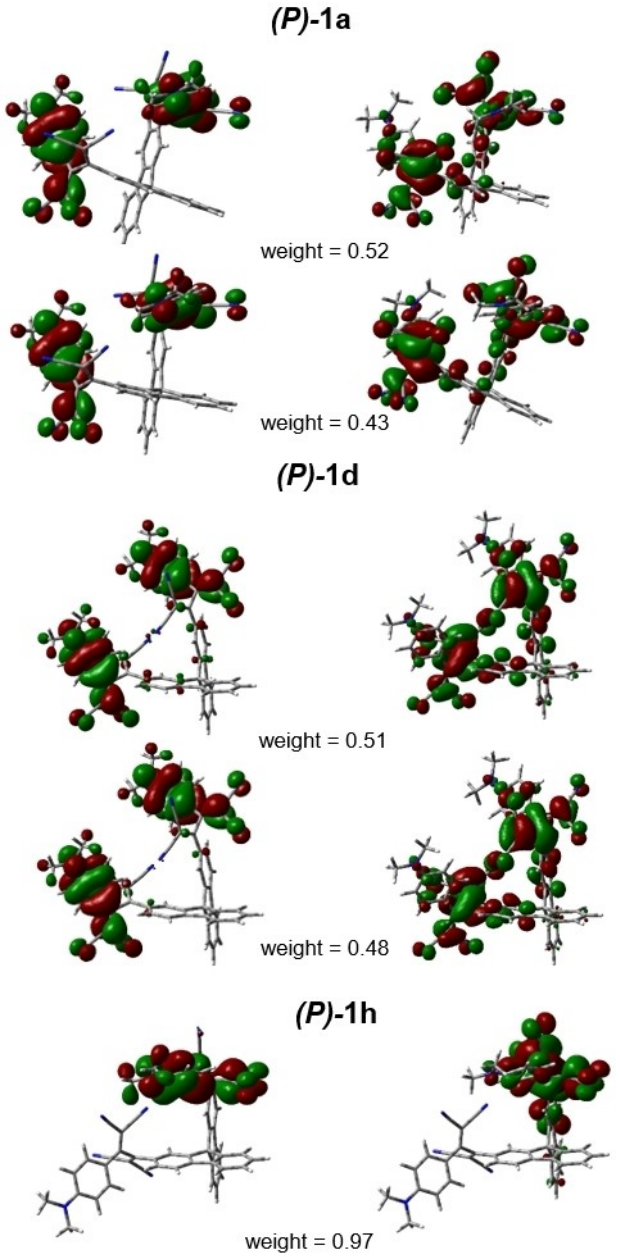

Figure 5. Dominant NTO pairs that contribute more than 50% to the lowest electronic transition (S1) of conformations (*P*)-**1 a**, (*P*)-**1 d** and (*P*)-**1 h** computed at the CAM-B3LYP level of theory using 6-31G(d,p) basis set with an isosurface value of 0.02 electrons/bohr^3.

unambiguously the (*P*) absolute configuration for fraction B of **1**.

With the goal of analyzing the NLO properties of (*P*)-**1**, we calculated the first hyperpolarizabilities for the three more stable conformations (*P*)-**1 a**, (*P*)-**1 d** and (*P*)-**1 h**. While conformer (*P*)-**1 h** bears the highest first hyperpolarizability, 84.4 10^{-30} esu, this value is 17.3×10^{-30} esu for (*P*)-**1 d**, and 3.8×10^{-30} esu for (*P*)-**1 a** (more details are given in the Supporting Information). Remarkable differences in the hyperpolarizability values for the three structures were observed. It is well established that NLO properties are associated with intramolecular charge transfer (ICT) process.[6] Therefore, the analysis of the charge transfer in the three structures seems to be essential. In literature, frontier molecular orbitals (FMOs) and natural transitions orbitals (NTOs) have been employed to study and visualize the ICT.[34–36] Even

some studies have shown a correlation between the HOMO-LUMO gap and hyperpolarizabilities and ICT.[36–38]

Frontier molecular orbitals and HOMO-LUMO gap for the three conformers were collected in the Supporting Information and NTOs for the first and second dominant electronic transitions were visualized at the CAM-B3LYP/6-31G(d,p) (Figure 5). In general, NTOs are obtained by transforming the canonical molecular orbitals into a more compact form and they are a useful tool to describe electronic transitions and CT.[39] For (*P*)-**1 a** and (*P*)-**1 d**, intramolecular charge transfer (ICT)[6] occurs simultaneously in both halves of the molecule between the aniline and the TCBD moieties for the two lowest electronic transitions, yet the two lowest electronic transitions represent an ICT in only one of the arms of the system in the case of (*P*)-**1 h**. NTOs, FOMs and HOMO-LUMO gaps show a more efficient intramolecular charge transfer in the (*P*)-**1 h** (for more details see the Supporting Information). We believe that this is the reason why (*P*)-**1 h** presents much larger hyperpolarizabilities than the other two stable conformations.

Conclusion

In summary, we have synthesized the first SBF-TCBD derivative (±)-**1** via click reaction between electron-rich alkyne (±)-**2** and TCNE as a strong electron acceptor. HPLC-CSP method successfully has provided the enantiomers of **1** in a high enantiomeric excess. Comprehensive PES analyses and subsequent ECD spectra simulations at the B3LYP/6-31G(d,p) level of theory have enabled us to assign unambiguously the AC of each fraction collected from HPLC. Theoretical calculations also have pointed out that the first hyperpolarizability values of the most stable conformers dramatically differ and this fact could be explained in terms of more intense ICT transitions in (*P*)-**1 h** because of its lower symmetry. The predicted first hyperpolarizability values of conformers (*P*)-**1 a** and (*P*)-**1 h** are higher than the previously reported allene-based analogue,[6] especially it becomes remarkable for (*P*)-**1 h**. We believe that this study can provide the framework for developing novel TCBD-SBF derivatives suitable for NLO applications.

Experimental Section

General information

All reagents were commercially available compounds of the highest purity. HPLC grade solvents were used for the HPLC method. Flash column chromatography (FCC) was carried out using Merck silica gel 60 (230–400 mesh) under pressure. Analytical thin layer chromatography (TLC) was performed on aluminum plates with silica gel Macherey-Nagel UV_{254} and visualized by UV irradiation (254 nm) or 365 nm or by staining with a solution of phosphomolybdic acid. HPLC was performed using the separations module Waters 2695, the photoiode array detector Waters 996 and the chiral stationary phase Chiralpak® IA (Daicel Chemical Industries Ltd.). UV/Vis and ECD spectra were recorded on a Jasco J-815 spectropolarimeter at 25 °C employing 1 cm cuvette. ^{1}H NMR and ^{13}C NMR spectra were recorded in $CDCl_3$ at 25 °C on a Bruker AMX-400 spectrometer operating at 400.16 MHz and 100.62 MHz with residual protic solvent as the internal references ^{1}H = 7.26 ppm and ^{13}C = 77.16 ppm. Chemical shifts (δ) are given in parts per million (ppm) and coupling constants (*J*) are given in Hertz (Hz). The spectra are reported as follows: δ (multiplicity, coupling constant *J*, number of protons and assignment). HR-ESI-MS spectrum was measured with an APEX3 instrument. Thermal stability was studied by simultaneous thermogravimetric analysis (TGA) and differential scanning calorimetry (DSC) using a Setaram SETSYS Evolution 1750 instrument.

1,1,4,4-tetracyanobutadiene spirobifluorene (±)-**1**: Into a 5 mL vial, SBF (±)-**2** (9.3 mg, 0.015 mmol) and tetracyanoethylene (5 mg, 0.040 mmol) were added and dissolved in $CDCl_3$ (1.5 mL) and stirred for 5 h at 25 °C. After evaporating the solvent, the purification of the crude by flash column chromatography (SiO_2, gradient from 30 % to 60 % EtOAc/*n*-hexane) afforded (±)-**1** (12.9 mg, 100 %) as a brown solid. ^{1}H NMR (400.16 MHz, $CDCl_3$, δ): 7.95 (dd, *J* = 8.2, 0.6 Hz, 2H, H4 and H4′), 7.92 (ddd, *J* = 7.7, 1.2, 0.8 Hz, 2H, H5 and H5′), 7.69 (d, *J* = 9.4 Hz, 4H, H2″ and H6″), 7.5-7.4 (m, 4H, H3, H3′, H6 and H6′), 7.40 (*br* s, 2H, H1 and H1′), 7.28 (td, *J* = 7.7, 1.1 Hz, 2H, H7 and H7′), 6.76 (ddd, *J* = 7.7, 1.0, 0.7 Hz, 2H, H8 and H8′), 6.68 (d, *J* = 9.4, 4H, H3″ and H5″), 3.16 (s, 12H, 2x(N(C**H**$_3$)$_2$)) ppm. ^{13}C NMR (101.19 MHz, $CDCl_3$, δ): 168.6 (2x, SBF**C**(C)=C(CN)$_2$), 163.5 (2x, PhNMe$_2$**C**(C)=C-(CN)$_2$), 154.6 (2x, C4″), 148.9 (2x, C), 148.4 (2x, C), 148.3 (2x, C), 139.8 (2x, C), 132.8 (4x, C2″ and C6″), 131.5 (2x, C), 130.9 (2x, C3 and C3′), 130.8 (2x, C7 and C7'), 129.1 (2x, C6 and C6'), 125.1 (2x, C1 and C1'), 124.6 (2x, C8 and C8'), 121.9 (2x, C4 and C4' or C5 and C5'), 121.6 (2x, C4 and C4' or C5 and C5'), 118.6 (2x, C1''), 114.6 (2x, **C**≡N), 113.6 (2x, **C**≡N), 112.4 (6x, C3'', C5'' and **C**≡N), 111.7 (2x, **C**≡N), 85.8 (2x, C=C(C≡N)$_2$), 74.3 (2x, C=C(C≡N)$_2$), 65.9 (C9), 40.3 (4x, N(**C**H$_3$)$_2$) ppm. HR-ESI-MS: *m/z* calc. for $C_{57}H_{35}N_{10}$ $[(M+H)]^+$, 859.3041; found, 859.3016.

Computational methods

All computational theoretical calculations were performed using the GAUSSIAN 09 program package.[40] Computational data not indicated in the manuscript can be found in the Supporting Information.

Acknowledgements

This work was funded by Xunta de Galicia (ED431F2016/005 and GRC2019/24), IIS Galicia Sur, and IBEROS (0245_IBEROS_1_E). A.O. thanks Xunta de Galicia for predoctoral fellowship and New Materials Group (University of Vigo, Spain) for a research contract. The authors also gratefully acknowledge CACTI de Vigo. Funding for open access charge: Universidade de Vigo/CISUG

Conflict of Interest

The authors declare no conflict of interest.

Data Availability Statement

The data that support the findings of this study are available in the supplementary material of this article.

Keywords: Chirality · Enantiomeric Resolution · Spectroscopy · Spirobifluorenes · Tetracyanobutadiene

[1] Y. Si, G. Yang, Z. Su, *J. Mater. Chem. C* **2013**, *1*, 1399–1406.
[2] N. S. Labidi, *Int. J. Met.* **2013**, *2013*, 1–5.
[3] H. Wu, H. Yu, S. Pan, Z. Huang, Z. Yang, X. Su, K. R. Poeppelmeier, *Angew. Chem. Int. Ed.* **2013**, *52*, 3406–3410; *Angew. Chem.* **2013**, *125*, 3490–3494.
[4] B. J. Coe, J. Fielden, S. P. Foxon, B. S. Brunschwig, I. Asselberghs, K. Clays, A. Samoc, M. Samoc, *J. Am. Chem. Soc.* **2010**, *132*, 3496–3513.
[5] L. R. Dalton, P. A. Sullivan, D. H. Bale, *Chem. Rev.* **2009**, *110*, 25–55.
[6] Y. Si, G. Yang, *J. Phys. Chem. A* **2014**, *118*, 1094–1102.
[7] X. Wu, J. Wu, Y. Liu, A. K.-Y. Jen, *J. Am. Chem. Soc.* **1999**, *121*, 472–473.
[8] Y. Si, G. Yang, *J. Mater. Chem. C* **2013**, *1*, 2354–2361.
[9] A. Baeyer, *Ber. Dtsch. Chem. Ges.* **1900**, *33*, 3771–3775.
[10] T. P. I. Saragi, T. Spehr, A. Siebert, T. Fuhrmann-Lieker, J. Salbeck, *Chem. Rev.* **2007**, *107*, 1011–1065.
[11] M. Valášek, K. Edelmann, L. Gerhard, O. Fuhr, M. Lukas, M. Mayor, *J. Org. Chem.* **2014**, *79*, 7342–7357.
[12] D. Becker, N. Konnertz, M. Böhning, J. Schmidt, A. Thomas, *Chem. Mater.* **2016**, *28*, 8523–8529.
[13] Y. Ferrand, C. Poriel, P. Le Maux, J. Rault-Berthelot, G. Simonneaux, *Tetrahedron: Asymmetry* **2005**, *16*, 1463–1472.
[14] Q. Wang, F. Lucas, C. Quinton, Y. K. Qu, J. Rault-Berthelot, O. Jeannin, S. Y. Yang, F. C. Kong, S. Kumar, L. S. Liao, et al., *Chem. Sci.* **2020**, *11*, 4887–4894.
[15] C. Poriel, J. Lle Rault-Berthelot, *J. Mater. Chem. C* **2017**, *5*, 3869–3897.
[16] S. Castro-Fernández, M. M. Cid, C. S. López, J. L. Alonso-Gómez, *J. Phys. Chem. A* **2015**, *119*, 1747–1753.
[17] S. Castro-Fernández, R. Yang, A. P. García, I. L. Garzón, H. Xu, A. G. Petrovic, J. L. Alonso-Gómez, *Chem. Eur. J.* **2017**, *23*, 11747–11751.
[18] A. Ozcelik, Á. Peña-Gallego, R. Pereira-Cameselle, J. L. Alonso-Gómez, *Chirality* **2020**, *32*, 464–473.
[19] A. Ozcelik, D. Aranda, S. Gil-Guerrero, X. A. Pola-Otero, M. Talavera, L. Wang, S. K. Behera, J. Gierschner, Á. Peña-Gallego, F. Santoro, R. Pereira-Cameselle, J. L. Alonso-Gómez, *Chem. Eur. J.* **2020**, *26*, 17342–17349.
[20] T. Michinobu, J. C. May, J. H. Lim, C. Boudon, J.-P. Gisselbrecht, P. Seiler, M. Gross, I. Biaggio, F. Diederich, *Chem. Commun.* **2005**, 737–739.
[21] M. Sekita, B. Ballesteros, F. Diederich, D. M. Guldi, G. Bottari, T. Torres, *Angew. Chem. Int. Ed.* **2016**, *55*, 5560–5564; *Angew. Chem.* **2016**, *128*, 5650–5654.
[22] R. García, J. Calbo, R. Viruela, M. Á. Herranz, E. Ortí, N. Martín, *ChemPlusChem* **2018**, *83*, 300–307.
[23] C. Philippe, A. T. Bui, S. Batsongo-Boulingui, Z. Pokladek, K. Matczyszyn, O. Mongin, L. Lemiè, F. Paul, T. A. Hamlin, Y. Trolez, *Org. Lett.* **2021**, *23*, 2007–2012.
[24] G. Lavarda, N. Bhattacharjee, G. Brancato, T. Torres, G. Bottari, *Angew. Chem. Int. Ed.* **2020**, *59*, 21224–21229; *Angew. Chem.* **2020**, *132*, 21410–21415.
[25] J. L. Alonso-Gómez, P. Schanen, P. Rivera-Fuentes, P. Seiler, F. Diederich, *Chem. Eur. J.* **2008**, *14*, 10564–10568.
[26] J. L. Alonso-Gómez, A. G. Petrovic, N. Harada, P. Rivera-Fuentes, N. Berova, F. Diederich, *Chem. Eur. J.* **2009**, *15*, 8396–8400.
[27] R. Bouvier, R. Durand, L. Favereau, M. Srebro-Hooper, V. Dorcet, T. Roisnel, N. Vanthuyne, Y. Vesga, J. Donnelly, F. Hernandez, et al., *Chem. Eur. J.* **2018**, *24*, 14484–14494.
[28] A. Ozcelik, D. Aranda, R. Pereira-Cameselle, M. Talavera, B. Covelo, F. Santoro, Á. Peña-Gallego, J. L. Alonso-Gómez, *ChemPlusChem* **2022**, https://chemistry-europe.onlinelibrary.wiley.com/doi/10.1002/cplu.202100554..
[29] T. Michinobu, C. Boudon, J.-P. Gisselbrecht, P. Seiler, B. Frank, N. N. P. Moonen, M. Gross, F. Diederich, *Chem. Eur. J.* **2006**, *12*, 1889–905.
[30] N. Berova, K. Nakanishi, R. W. Woody, *Circular Dichroism: Principles and Applications*, Wiley, New York, **2000**, 55.
[31] D. Shcherbin, K. Ruud, *Chem. Phys.* **2008**, *349*, 234–243.
[32] A. Fortunelli, J. Tomasi, *Chem. Phys. Lett.* **1994**, *231*, 34–39.
[33] A. G. Petrovic, A. Navarro-Vázquez, J. L. Alonso-Gómez, *Curr. Org. Chem.* **2010**, *14*, 1612–1628.
[34] B. Kharat, M. Naganathappa, V. Jagrut, A. Chaudhari, *Spectrochim. Acta Part A* **2022**, *265*, 120389.
[35] F. K. Bine, N. S. Tasheh, J. N. Ghogomu, F. K. Bine, N. S. Tasheh, J. N. Ghogomu, *Comput. Chem.* **2021**, *9*, 215–237.
[36] N. K. Nkungli, J. N. Ghogomu, *J. Theor. Chem.* **2016**, *2016*, 1–19.
[37] C. C. Fonkem, G. W. Ejuh, F. T. Nya, R. A. Y. Kamsi, Y. T. Assatse, J. M. B. Ndjaka, *Chin. J. Phys.* **2020**, *63*, 207–212.
[38] S. R. Sapale, N. A. Borade, *Eur. J. Mol. Clin. Med.* **2020**, *7*, 4529–4539.
[39] R. L. Martin, *J. Chem. Phys.* **2003**, *118*, 4775–4777.
[40] Gaussian Revision C.01 M. J. Frisch, G. W. Trucks, H. B. Schlegel, G. E. Scuseria, M. A. Robb, J. R. Cheeseman, G. Scalmani, V. Barone, G. A. Petersson, H. Nakatsuji, X. Li, M. Caricato, A. V. Marenich, J. Bloino, B. G. Janesko, R. Gomperts, B. Mennucci, H. P. Hratchian, J. V. Ortiz, A. F. Izmaylov, J. L. Sonnenberg, D. Williams-Young, F. Ding, F. Lipparini, F. Egidi, J. Goings, B. Peng, A. Petrone, T. Henderson, D. Ranasinghe, V. G. Zakrzewski, J. Gao, N. Rega, G. Zheng, W. Liang, M. Hada, M. Ehara, K. Toyota, R. Fukuda, J. Hasegawa, M. Ishida, T. Nakajima, Y. Honda, O. Kitao, H. Nakai, T. Vreven, K. Throssell, J. A. Montgomery, Jr., J. E. Peralta, F. Ogliaro, M. J. Bearpark, J. J. Heyd, E. N. Brothers, K. N. Kudin, V. N. Staroverov, T. A. Keith, R. Kobayashi, J. Normand, K. Raghavachari, A. P. Rendell, J. C. Burant, S. S. Iyengar, J. Tomasi, M. Cossi, J. M. Millam, M. Klene, C. Adamo, R. Cammi, J. W. Ochterski, R. L. Martin, K. Morokuma, O. Farkas, J. B. Foresman, D. J. Fox, Gaussian Inc., Wallingford CT, **2016**..

Manuscript received: November 1, 2021
Revised manuscript received: March 25, 2022
Accepted manuscript online: March 30, 2022